AAC Journals.ASM.org

Cyclopalladated Compound 7a Induces Apoptosis- and Autophagy-Like Mechanisms in *Paracoccidioides* and Is a Candidate for Paracoccidioidomycosis Treatment

Denise C. Arruda,[a,c] Alisson L. Matsuo,[a] Luiz S. Silva,[a] Fernando Real,[a] Natanael P. Leitão, Jr.,[a] Jhon H. S. Pires,[a] Antonio Carlos F. Caires,[b†] Daniel M. Garcia,[b] Fernanda F. M. Cunha,[c] Rosana Puccia,[a] Larissa V. G. Longo[a]

Departamento de Microbiologia, Imunologia e Parasitologia, Escola Paulista de Medicina-Universidade Federal de São Paulo, EPM-UNIFESP, São Paulo, SP, Brazil[a]; Centro Interdisciplinar de Investigação Bioquímica, Universidade de Mogi das Cruzes, UMC, Mogi das Cruzes, SP, Brazil[b]; Núcleo Integrado de Biotecnologia, Universidade de Mogi das Cruzes, UMC, Mogi das Cruzes, SP, Brazil[c]

Paracoccidioidomycosis (PCM), caused by *Paracoccidioides* species, is the main cause of death due to systemic mycoses in Brazil and other Latin American countries. Therapeutic options for PCM and other systemic mycoses are limited and time-consuming, and there are high rates of noncompliance, relapses, toxic side effects, and sequelae. Previous work has shown that the cyclopalladated 7a compound is effective in treating several kinds of cancer and parasitic Chagas disease without significant toxicity in animals. Here we show that cyclopalladated 7a inhibited the *in vitro* growth of *Paracoccidioides lutzii* Pb01 and *P. brasiliensis* isolates Pb18 (highly virulent), Pb2, Pb3, and Pb4 (less virulent) in a dose-response manner. Pb18 was the most resistant. Opportunistic *Candida albicans* and *Cryptococcus neoformans* were also sensitive. BALB/c mice showed significantly lighter lung fungal burdens when treated twice a day for 20 days with a low cyclopalladated 7a dose of 30 μg/ml/day for 30 days after intratracheal infection with Pb18. Electron microscopy images suggested that apoptosis- and autophagy-like mechanisms are involved in the fungal killing mechanism of cyclopalladated 7a. Pb18 yeast cells incubated with the 7a compound showed remarkable chromatin condensation, DNA degradation, superoxide anion production, and increased metacaspase activity suggestive of apoptosis. Autophagy-related killing mechanisms were suggested by increased autophagic vacuole numbers and acidification, as indicated by an increase in LysoTracker and monodansylcadaverine (MDC) staining in cyclopalladated 7a-treated Pb18 yeast cells. Considering that cyclopalladated 7a is highly tolerated *in vivo* and affects yeast fungal growth through general apoptosis- and autophagy-like mechanisms, it is a novel promising drug for the treatment of PCM and other mycoses.

Paracoccidioidomycosis (PCM) is a systemic granulomatous mycosis caused by *Paracoccidioides brasiliensis* and *Paracoccidioides lutzii*. It is geographically restricted to Central and South America, with a high incidence in Brazil, Colombia, Venezuela, and Argentina (1). PCM has the highest mortality rate among systemic mycoses in Brazil, which has been estimated to be 1.45 per million inhabitants. It affects mainly males engaged in agricultural activities because they inhale aerosols containing fungal conidia while working the soil (1). *P. brasiliensis* and *P. lutzii* are thermal dimorphic fungi that grow as yeast-like cells at 37°C and as mycelia at mild temperatures below 26°C. Upon inhalation by human hosts, conidia transform into multibudding yeast cells in the pulmonary alveoli in response to the temperature increase. The pathogenic yeast cells affect mainly the lungs, although disseminated disease can also occur. PCM progression depends on many factors but especially on the host immune response and fungal virulence (2).

The incidence of mycoses, which vary from superficial and cutaneous to systemic and invasive, has increased dramatically in the past decades, especially in immunocompromised individuals. Mild and moderate forms of PCM are usually treated with itraconazole or a combination of sulfamethoxazole and trimethoprim. However, it has recently been shown that itraconazole induces an earlier clinical cure and is better tolerated than sulfamethoxazole-trimethoprim (3, 4). For severe and disseminated cases, amphotericin B deoxycholate is the drug of choice, even considering its known adverse effects, especially nephrotoxicity (5). Nanostructured formulations of drugs, such as liposomes and polymeric nanoparticles, have greatly improved the pharmacological response by allowing slow and gradual drug release, thus reducing toxicity (6). Less toxic amphotericin B nanostructured lipid formulations are available but at high cost. Despite the clinically available antifungal drugs, relapses and/or sequelae (fibrosis) are still problems in PCM treatment (7). Therefore, new strategies aiming at the immune therapy of experimental PCM have been tested. The best-studied antigen for this purpose is gp43 (8), but therapy with a recombinant hsp65 DNA has also decreased fungal burdens and reduced fibrosis formation in a PCM experimental murine model (9). The gp43 main T-cell epitope is a 15-amino-acid-long peptide named P10 that potentiates the effectiveness of fungicidal drugs like itraconazole and sulfamethoxazole-trimethoprim by boosting a Th1-driven immune response (10).

Received 3 March 2015 **Returned for modification** 4 May 2015
Accepted 26 August 2015

Accepted manuscript posted online 8 September 2015

Citation Arruda DC, Matsuo AL, Silva LS, Real F, Leitão NP, Jr, Pires JHS, Caires ACF, Garcia DM, Cunha FFM, Puccia R, Longo LVG. 2015. Cyclopalladated compound 7a induces apoptosis- and autophagy-like mechanisms in *Paracoccidioides* and is a candidate for paracoccidioidomycosis treatment. Antimicrob Agents Chemother 59:7214–7223. doi:10.1128/AAC.00512-15.

Address correspondence to Rosana Puccia, ropuccia@gmail.com.

† Deceased.

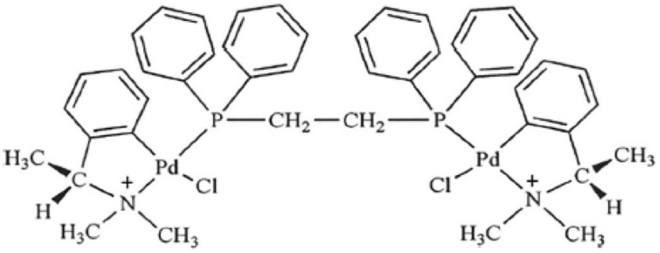

FIG 1 Molecular structure of the cyclopalladated 7a compound $[Pd_2(S(-)C_2,N\text{-DMPA})_2(m\text{-DPPE})]Cl_2$.

Recently, cyclopalladated complexes with biological activity have been shown to be more stable and less toxic than other palladium-containing compounds (11). One of these compounds, $[Pd_2(S(-)C_2,N\text{-DMPA})_2(m\text{-DPPE})]Cl_2$, named 7a, was effective at low concentrations *in vitro* and *in vivo* against different infectious and noninfectious diseases reproduced in animal models. More importantly, the compound was not toxic to animals when 100 μl of a 150-μg/ml solution was administered for 5 sequential days (data not shown). Cyclopalladated 7a was effective in the treatment of murine melanoma (12) and human melanoma, colon, breast, and uterine cervix cancers; glioblastoma (13); leukemia (14); and Chagas disease (15). In tumor cells, cyclopalladated 7a causes anoikis and apoptosis by dissipating the mitochondrial membrane potential, thus activating effector caspases, causing chromatin condensation and DNA degradation (13, 14). In *Trypanosoma cruzi*, which causes Chagas disease, cyclopalladated 7a evokes an apoptosis-like cell death through mitochondrial disruption (15).

We show here that cyclopalladated 7a is effective against the yeast phase of *Paracoccidioides in vitro* and *in vivo*. The mechanism of action seems to involve both apoptosis- and autophagy-like mechanisms. Our results suggest that cyclopalladated 7a is a promising drug for the treatment of PCM and also potentially of candidiasis and cryptococcosis.

MATERIALS AND METHODS

Fungal growth conditions. *P. lutzii* Pb01 and *P. brasiliensis* isolates Pb3, Pb18, Pb2, and Pb4 were cultivated as previously described (16). Fungal yeast cells were cultivated for 7 days at 36°C on modified YPD (0.5% yeast extract, 0.5% casein peptone, 1.5% glucose, pH 6.5) slants and seeded into 50 ml of Ham's F12 medium (Life Technologies, Grand Island, NY, USA) supplemented with 1.5% glucose (F12/Glc) for preinoculum growth for 4 days while shaking at 36°C. The combined cells from four preinocula were then transferred to fresh F12/Glc (200 ml) and cultivated for 2 days under the same conditions. Viability (>95%) was estimated by trypan blue staining. *Candida albicans* and *Cryptococcus neoformans* were maintained at 36°C on modified YPD medium slants. For experimental purposes, they were transferred to liquid medium and cultivated for 2 days in F12/Glc at 36°C while shaking.

Animals. BALB/c male mice (8 to 10 weeks old) were purchased from CEDEME (Centro de Desenvolvimento de Modelos Experimentais, UNIFESP) and maintained in a sterilized environment with 12-h light-dark cycles. All of the animal experiments and procedures were done in accordance with the ethical handling of laboratory animals and were approved by the UNIFESP Animal Experimentation Ethics Committee (protocol 0366/07).

Cyclopalladated compound 7a. Palladacycle compound 7a was synthesized from *N*,*N*-dimethyl-1-phenethylamine (DMPA) complexed with the ligand 1,2-ethane-bis(diphenylphosphine) (DPPE) as previously described (12). For this work, a 1 mM stock solution of 7a was prepared with 1% dimethyl sulfoxide in 50 mM phosphate buffer, and the drug was further diluted to the appropriate concentration in phosphate-buffered saline (PBS) (12).

***in vitro* yeast viability assay.** *Paracoccidioides*, *C. albicans*, and *C. neoformans* yeast cells were counted in a Neubauer chamber, and 1.2×10^4 cells were incubated overnight at 37°C with 1 ml of cyclopalladated 7a (0.08 to 10 μg/ml) or PBS (negative control). An aliquot (200 μl) of the suspension was plated onto brain heart infusion (BHI) medium (Difco, Sparks, MD, USA) supplemented with 4% fetal calf serum and 5% spent *P. brasiliensis* culture medium (17) for *P. brasiliensis* or modified YPD for *C. albicans* and *C. neoformans*. The plates were incubated at 37°C, and *C. albicans*, *C. neoformans* and *P. brasiliensis* CFU counts were recorded after 2, 4, and 14 days, respectively. We recorded the lowest concentrations yielding 50 and 90% CFU count reductions. All of the experiments were performed in triplicate.

Treatment of experimental PCM with cyclopalladated 7a. BALB/c mice (nine per group) were intratracheally infected with Pb18 (1×10^6 yeast cells), and after 30 days, when experimental PCM was established (18), the animals were treated twice a day for 20 days with 100-μl intraperitoneal doses of cyclopalladated 7a (15 μg/ml/dose). PBS was used as a negative control. After 60 days of infection, the lungs were collected, macerated in PBS, and plated in supplemented BHI medium. Colony numbers were counted after 14 days of incubation at 37°C and recorded as the number of CFU per gram of lung tissue.

Histopathological analysis. The lungs of PBS- and cyclopalladated 7a-treated BALB/c mice were excised, fixed in PBS–10% formalin, dehydrated, and embedded in paraffin. Five-micrometer sections of tissue were stained with hematoxylin-eosin and Grocott stain, and lung lesions were observed with an Olympus BX-51 microscope. For toxicological analysis, 150 μg/ml cyclopalladated 7a (100 μl) was administered for 5 sequential days to three BALB/c mice, and sections of kidney, liver, heart, lung, and spleen tissues were stained with hematoxylin-eosin and analyzed in comparison with control tissues.

Detection of DNA fragmentation. Terminal deoxynucleotidyltransferase (TdT)-mediated dUTP-biotin nick end labeling (TUNEL) assays were performed according to the manufacturer's instructions (*In Situ* Cell Death Detection kit, fluorescein; Roche Applied Science, Indianapolis, IN, USA). Briefly, Pb18 yeast cells were incubated for 18 h at 37°C with cyclopalladated 7a (1 μg/ml), washed, fixed in 2% formaldehyde, and permeabilized with 0.1% Triton X-100 for 30 min at room temperature. Fixed cells were stained with 4′,6-diamidino-2-phenylindole (DAPI; 1 μg/ml) for 20 min and incubated with TdT in the reaction buffer with dUTP-fluorescein at 37°C for 1 h. Cells were then washed in PBS, prepared on glass slides with Vectashield mounting medium (Vector Labo-

TABLE 1 Effects of cyclopalladated 7a on the *in vitro* growth of *C. albicans*, *C. neoformans*, and *Paracoccidioides* isolates[a]

Isolate	Concn (μg/ml) required to reduce CFU count by:	
	50%	90%
C. albicans	0.35	0.55
C. neoformans	0.3	0.57
P. brasiliensis Pb3	0.43	0.74
P. brasiliensis Pb18	0.41	0.76
P. lutzii Pb01	0.21	0.45
P. brasiliensis Pb2	0.05	0.12
P. brasiliensis Pb4	0.04	0.1

[a] Fungal yeast cells were incubated overnight at 37°C with cyclopalladated 7a at different concentrations. CFU of *C. albicans*, *C. neoformans*, and *P. brasiliensis* were counted after 2, 4, and 14 days, respectively. The lowest cyclopalladated 7a concentrations that yielded 50 and 90% reductions in CFU counts relative to those of PBS-treated controls were calculated.

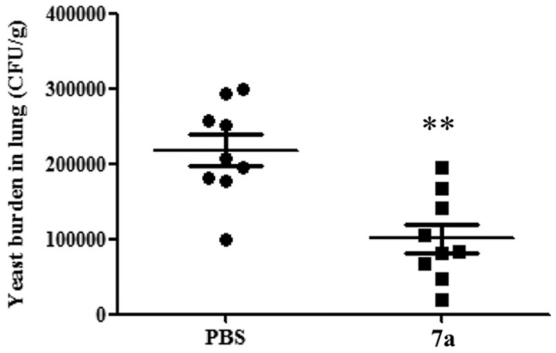

FIG 2 Cyclopalladated 7a affects the *in vivo* growth of virulent Pb18. BALB/c mice infected with *P. brasiliensis* (Pb18) yeast cells for 30 days were treated for 20 days with cyclopalladated 7a. Numbers of CFU per gram of lung tissue were determined 60 days after infection. The data represent the CFU counts of individual mice, and the horizontal bars show the means ± the standard deviations. Cyclopalladated 7a-treated mice were compared to PBS-treated controls. **, statistically significant ($P = 0.0031$).

ratories, Inc., Burlingame, CA), sealed, and observed with an Olympus BX-51 fluorescence microscope. Images were merged, and scale bars were added with the ImageJ software. Negative-control cells were incubated with PBS.

Chromatin condensation. Chromatin condensation was evaluated following Hoechst 33342 staining. Pb18 yeast cells were incubated for 18 h at 37°C with cyclopalladated 7a (1 μg/ml), washed in PBS, and fixed for 30 min at room temperature in 2% formaldehyde. Fixed cells were washed in PBS and stained with 0.2 μM Hoechst 33342 (Invitrogen, Grand Island, NY, USA) for 10 min. Cells were mounted on glass slides with Vectashield (Vector Laboratories, Inc., Burlingame, CA), sealed, and observed with an Olympus BX-51 fluorescence microscope. Scale bars were added with the ImageJ software. Negative-control cells were incubated with PBS.

Metacaspase activity. Metacaspase activity was estimated with CaspACE–fluorescein isothiocyanate (FITC)-VAD-FMK *In Situ* Marker (Promega, Madison, WI, USA) according to the manufacturer's instructions. Briefly, Pb18 yeast cells were incubated with cyclopalladated 7a (1 μg/ml) or PBS (negative control) for 18 h at 37°C and stained with CaspACE–FITC-VAD-FMK (10 μM) for 30 min at 37°C. The cells were then washed with PBS and fixed with 10% buffered formalin for 30 min at room temperature. Positive-control cells were previously treated with 2

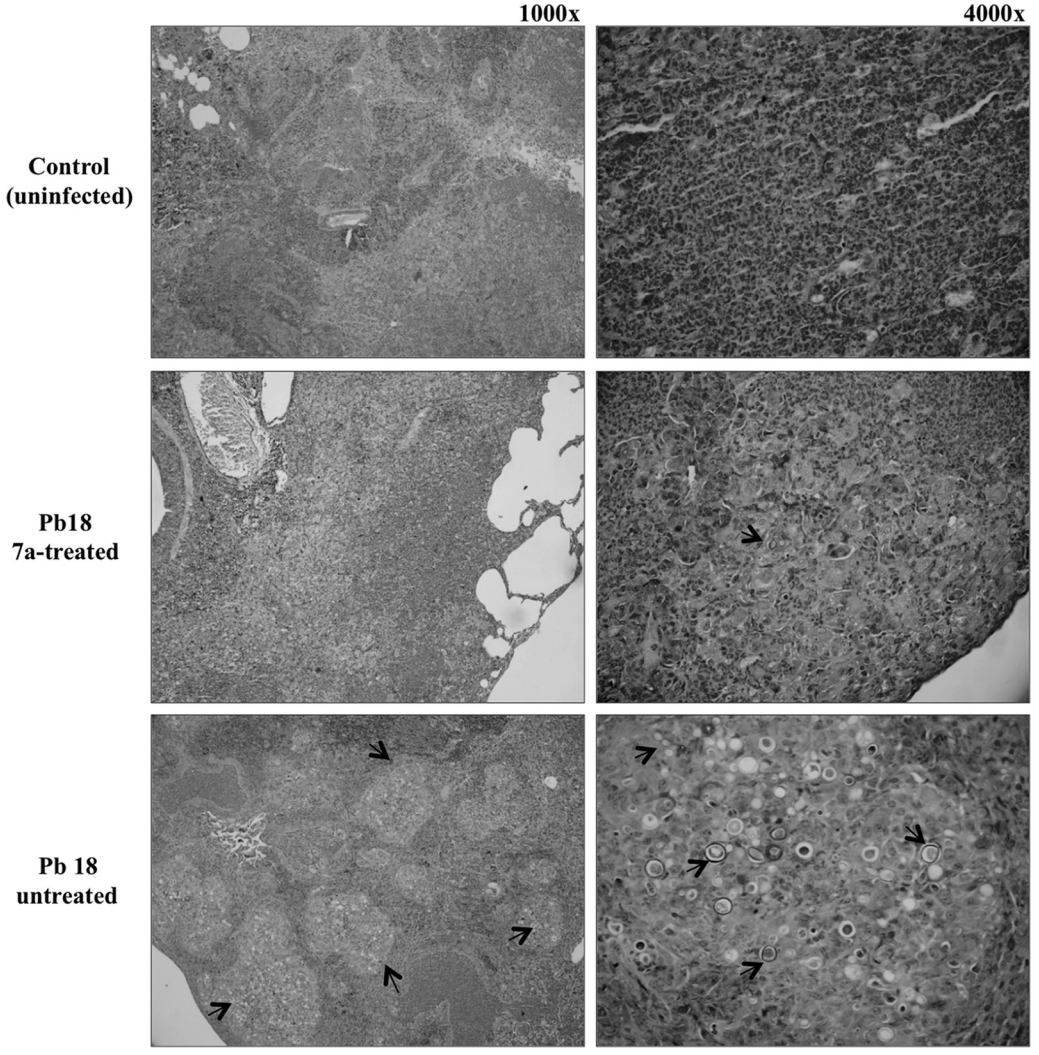

FIG 3 Lung histopathology analysis of cyclopalladated 7a-treated mice shows light fungal burdens. Hematoxylin-eosin-Grocott staining was used. BALB/c mice infected with Pb18 yeast cells for 30 days were treated with cyclopalladated 7a. Treated lungs are shown (magnifications, ×1,000 and ×4,000) in comparison with untreated and uninfected lungs. Granulomas (magnification, ×1,000) and yeast cells (magnification, ×4,000) are indicated by arrows.

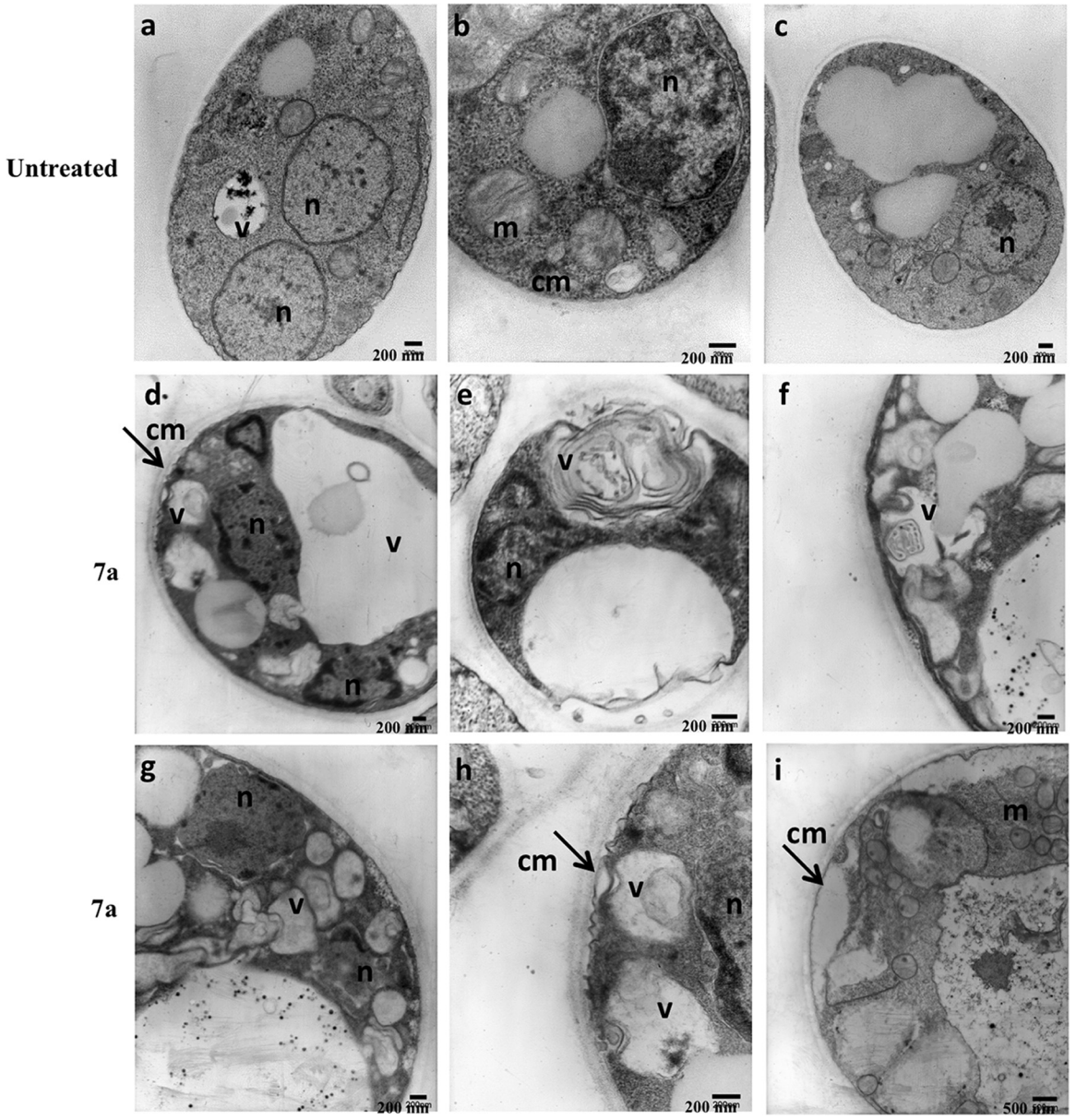

FIG 4 TEM images suggest apoptosis- and autophagy-like events in Pb18 yeast cells treated with cyclopalladated 7a. Different *P. brasiliensis* yeast cell images are shown before (a to c) and after (d to i) exposure to cyclopalladated 7a for 18 h. The vacuole (v), nucleus (n), mitochondrion (m), and cell membrane (cm) are indicated. The arrows show cell membrane disruption.

mM H_2O_2 at 37°C for 2 h. The samples were mounted on glass slides with Vectashield (Vector Laboratories, Inc., Burlingame, CA), sealed, and observed with an Olympus BX-51 fluorescence microscope. Scale bars were added with the ImageJ software.

Superoxide anion measurement. Superoxide anion production was measured with the dihydroethidium (DHE) assay according to the manufacturer's instructions (Invitrogen, Grand Island, NY, USA). Briefly, Pb18 yeast cells were incubated with cyclopalladated 7a (1 μg/ml) or PBS (negative control) for 18 h at 37°C and incubated with 5 μM DHE at room temperature for 30 min. The conversion of DHE to ethidium by oxidation was detected by fluorescence microscopy. Scale bars were added with the ImageJ software. Positive-control cells were previously treated with 2 mM H_2O_2 at 37°C for 2 h.

TEM. Pb18 yeast cells were incubated with cyclopalladated 7a (1 μg/ml) or PBS (negative control) for 18 h at 37°C and fixed in a solution containing 2.5% glutaraldehyde and 2% formaldehyde in 0.1 M sodium cacodylate buffer, pH 7.2, at room temperature for 20 h. The cells were washed in the same buffer for 10 min, fixed with 1% osmium tetroxide in 0.1 M cacodylate (pH 7.2) for 30 min, and washed in water for 10 min at room temperature. Subsequently, the cells were incubated in an aqueous solution of 0.4% uranyl acetate for 30 min and washed in water for 10 min. After fixation, the cells were dehydrated in graded (70, 90, and 100%) ethanol, quickly treated with propylene oxide, and embedded in Spurr resin. Ultrathin sections were collected on grids and stained in alcoholic 1% uranyl acetate and in lead citrate prior to analysis by transmission electron microscopy (TEM) with a 1200 EXII microscope (JEOL, Tokyo, Japan).

Live-cell imaging for quantification of acidic vesicles. For lysosomal quantification in live samples, Pb18 yeast cell walls were first stained with calcofluor white (25 μM) for 30 min at room temperature. The cells were

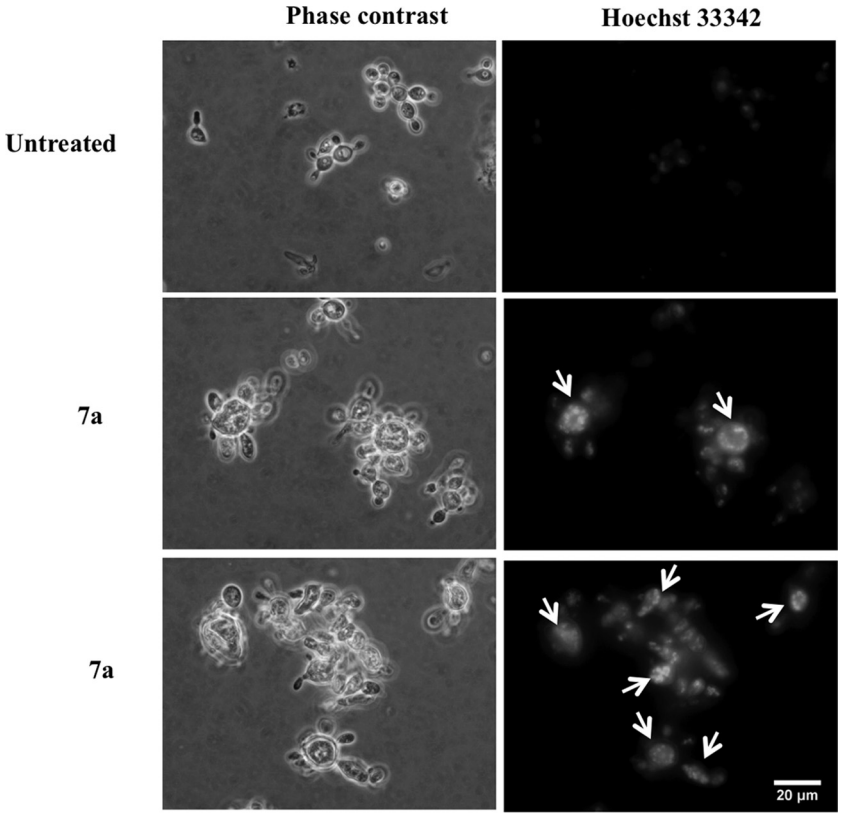

FIG 5 Cyclopalladated 7a induces chromatin condensation in *P. brasiliensis*. Pb18 yeast cells were treated with cyclopalladated 7a for 18 h, and chromatin condensation (arrows) was analyzed by fluorescence microscopy after DNA staining with Hoechst 33342. Phase-contrast images of the same fields are shown. Untreated cells are shown for comparison.

washed in PBS and allowed to adhere to a poly-L-lysine (Sigma-Aldrich, St. Louis, MO, USA)-pretreated plate. Nonadherent yeast cells were washed away with PBS. At that point, 5 μM LysoTracker Red (LTR) DND-99 (Life Technologies, Grand Island, NY, USA) and cyclopalladated 7a (1 μg/ml) were added to the samples for live-cell imaging in a Leica TCS SP5 confocal microscope coupled to microincubators set to 37°C. Live-cell imaging was performed with Hi-Q4 multichamber dishes that allowed 24-h acquisition of images of duplicate samples of cells treated with cyclopalladated 7a or not treated. The time interval between image acquisitions was set to 15 or 20 min. Four different microscopic fields of each sample were recorded. Live-cell serial images were processed by Imaris software (Bitplane) as follows on the basis of methods previously established (19). Isosurfaces were constructed on the basis of the calcofluor signal, which allowed the assessment of several morphological parameters, such as volume, area, and relative fluorescence intensity. The constructed isosurfaces may include several or individual yeast cells in each microscopic field. To infer and compare the amount of acidic compartments displayed by yeast cells treated with cyclopalladated 7a or not treated, the relative fluorescence intensity of the LysoTracker probe contained within each calcofluor-derived isosurface was normalized per unit of isosurface volume.

Live-cell imaging for quantification of autophagic vesicles. For quantification of autophagic vesicles in live samples, we reproduced the experiments detailed above with lysosomes and different fluorescent compounds. Briefly, plates containing adherent Pb18 yeast cells were recorded as described for live-cell imaging in the presence of 20 μM monodansylcadaverine (MDC) and cyclopalladated 7a (1 μg/ml). In the image-processing steps, the isosurfaces were constructed from the CellTracker Red CMTPX Dye (Life Technologies, Grand Island, NY, USA) signal and the relative fluorescence intensity of MDC displayed by each isosurface was assessed. The relative fluorescence intensities of MDC were also normalized per unit of isosurface volume.

Statistical analyses. The Student *t* test and one-way analysis of variance were used for statistical analyses.

RESULTS

Cyclopalladated 7a inhibits *Paracoccidioides* isolate growth *in vitro*. To evaluate the effect of cyclopalladated 7a (Fig. 1) on pathogenic fungal yeast cells, we performed *in vitro* CFU assays (Table 1) with *P. lutzii* Pb01 and *P. brasiliensis* isolate Pb18, Pb2, Pb3, and Pb4 yeast cells. In the *P. brasiliensis* complex, Pb18 represents major phylogenetic group S1 and is highly virulent, while Pb2, Pb3, and Pb4 represent cryptic group PS2 of less virulent isolates (17, 20). Dose-response experiments showed that, under the conditions used, the 7a compound was able to reduce the growth of all of the fungal isolates tested by 50% at low concentrations varying from 0.04 (Pb4) to 0.41 (Pb18) μg/ml. We also later tested the ability of cyclopalladated 7a to interfere with the cell growth of the opportunistic species *C. albicans* and *C. neoformans* with similar results (Table 1), suggesting that the compound acts on a broad spectrum of pathogenic yeast cells.

Cyclopalladated 7a decreases *P. brasiliensis* loads *in vivo*. To evaluate whether cyclopalladated 7a could decrease *P. brasiliensis* fungal loads in experimental PCM, we infected BALB/c mice with the most virulent isolate in our sample, i.e., Pb18. We then treated the animals with the cyclopalladated 7a compound twice a day for 20 days. Treatment started after 30 days of infection, when chronic PCM is stablished in BALB/c mice inoculated with Pb18 via the

intratracheal route (18). We analyzed the lungs of the mice, which are the target organs upon intratracheal inoculation. As shown in Fig. 2, cyclopalladated 7a-treated mice had a significantly lower mean number of CFU per gram of lung tissue (101,055) than control mice (218,111). These results resemble those described in the literature. Similar experiments with clinically available antifungal drugs (fluconazole, ketoconazole, itraconazole, amphotericin B, and sulfamethoxazole-trimethoprim) showed that there was generally a 50% reduction in the number of CFU of Pb18 per gram of treated mouse lung tissue (21), while amphotericin B caused an about 60% reduction. Representative images of the lung histopathology analysis results (Fig. 3) show that untreated animals had numerous granulomas filled with Pb18 yeast cells along the whole tissue. In treated animals, yeast cells were rarely seen and areas of fibrosis replaced the granulomas. Therefore, cyclopalladated 7a was able to decrease the lung fungal burdens and tissue damage caused by the fungal infection. It is of note that we used treatment doses that were much lower than toxic concentrations, considering that administration of 150 μg/ml of cyclopalladated 7a for 5 sequential days in BALB/c mice did not cause morphological alterations in the kidney, liver, heart, lung, or spleen tissue (data not shown). However, we have not tested further treatment protocols that could be more efficacious. After the above-described positive results, our focus became to understand the mechanism of action of the 7a compound on fungal cells.

Cell damage caused by cyclopalladated 7a. We used TEM to evaluate the type of damage caused by cyclopalladated 7a in *P. brasiliensis* yeast cells. Note that cyclopalladated 7a-treated yeast cells had organelle alterations suggestive of apoptosis-like and autophagy processes (Fig. 4d to i). Abnormal membrane structures inside vacuoles (Fig. 4d to h) also indicated a putative autophagy process. Mitochondrial swelling (Fig. 4i) and chromatin condensation (Fig. 4d, e, g, and h) suggested an apoptosis-like mechanism. Cell membrane disruption (Fig. 4d, e, h, and i, arrows) could also be seen. Considering these results, we further investigated whether apoptosis and autophagy could be involved in the mechanism of action of cyclopalladated 7a against *Paracoccidioides*.

Cyclopalladated 7a-induced apoptosis-like mechanisms. In order to evaluate whether an apoptosis-like mechanism is involved in the effect of cyclopalladated 7a on *P. brasiliensis*, we first investigated chromatin condensation. As shown in Fig. 5, incubation with cyclopalladated 7a induced remarkable chromatin condensation in comparison to control yeast cells, as shown by the bright spots inside the nuclei that are absent from control cells. Additionally, an intense DNA staining pattern was observed in the cytoplasm of cyclopalladated 7a-treated yeast cells, suggesting nucleic acid leakage caused by nuclear membrane disruption. Both chromatin condensation and nuclear membrane degradation were also observed in TEM images (Fig. 4).

DNA degradation is a classical apoptosis feature that has previously been caused by cyclopalladated 7a in other systems (12, 15). Thus, we evaluated the induction of DNA degradation in Pb18-treated yeast cells by TUNEL. Figure 6 shows that, in contrast to untreated cells, cyclopalladated 7a-treated yeast cells showed DNA breakage, evidenced by a green staining that colocalized with DAPI nuclear staining.

Considering that superoxide anion production during apoptosis has been well documented (22) and that we have observed mitochondrial swelling by TEM (Fig. 4i), we estimated the production of O_2^- anion in cyclopalladated 7a-treated cells and observed that it was dramatically increased, in a way that the fluorescence was even brighter than that induced by the H_2O_2-treated positive control (Fig. 7).

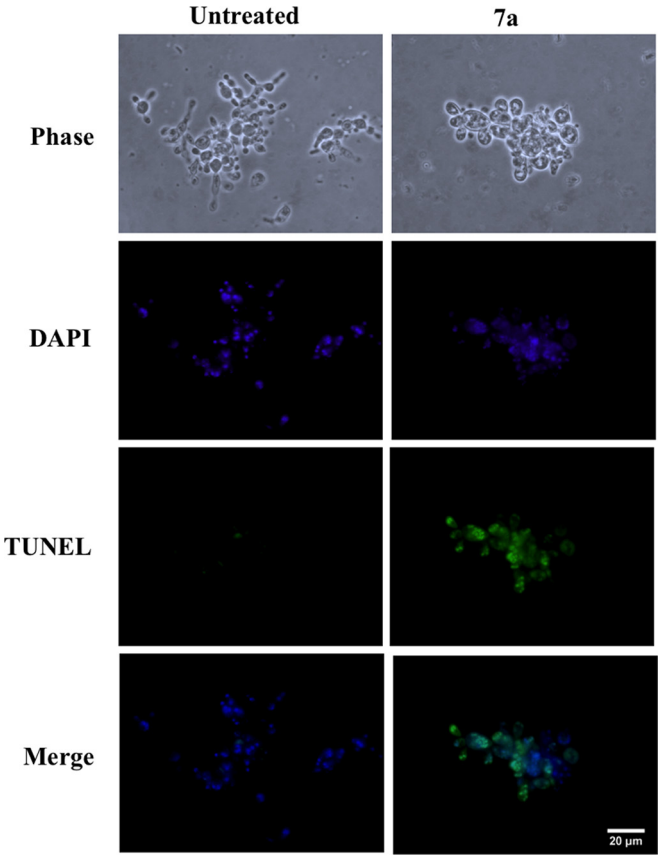

FIG 6 Cyclopalladated 7a induces DNA degradation in *P. brasiliensis*. Pb18 yeast cells were treated with cyclopalladated 7a for 18 h, and DNA degradation was observed by TUNEL in a fluorescence microscope. Images of treated (right) and control (left) cells obtained by phase-contrast microscopy, DAPI nuclear staining, and TUNEL are shown. Merged images of TUNEL and DAPI staining are also shown.

Apoptosis mechanisms in fungal cells are characterized by an increase in metacaspase activity (23). We evaluated metacaspase activity in *P. brasiliensis* yeast cells treated with cyclopalladated 7a by staining with the CaspACE–FITC-VAD-FMK reagent and observed a remarkable increase, which was even more intense than that of the positive control induced with H_2O_2 (Fig. 8). Together, these results strongly suggested that an apoptosis-like mechanism is involved in the *P. brasiliensis* killing mechanism of cyclopalladated 7a.

Cyclopalladated 7a induces autophagy-like events. TEM images suggested that autophagy-related processes are involved in the cyclopalladated 7a mechanism of action against *Paracoccidioides*. The methods used to assess autophagy rely on fluorescent tagging of acidic organelles with MDC or LTR (24). LTR stains endosomes, autophagosomes, lysosomes, and autolysosomes because of their low internal pH. To determine the concentration of LTR inside acidic lysosomes, we performed kinetic assays with a confocal microscope to monitor the acidification of *P. brasiliensis* organelles after contact with cyclopalladated 7a for 18 h (Fig. 9).

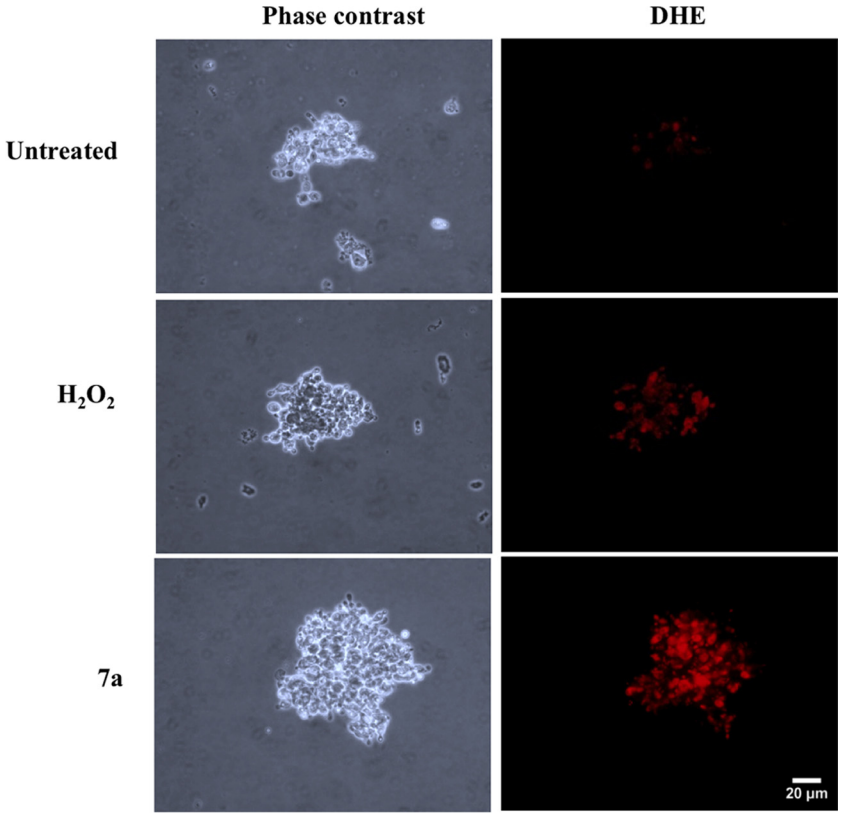

FIG 7 Cyclopalladated 7a induces anion superoxide production in *P. brasiliensis*. Pb18 yeast cells were treated with cyclopalladated 7a or H_2O_2 or left untreated for 18 h and stained with DHE. Induction of anion superoxide production was analyzed by fluorescence microscopy. Phase-contrast images are also shown.

As shown in Fig. 9A, a statistically significant increase in LTR fluorescence was observed in the cytoplasm during most of the time points during exposure to cyclopalladated 7a in comparison with controls (Fig. 9B). We then measured the proliferation of acidic organelles after exposure to cyclopalladated 7a by labeling with MDC, an autophagosomal marker. MDC is a weak amine that accumulates inside acidic organelles. Fluorescence is enhanced in hydrophobic environments characteristic of autophagic membranous organelles (25). In a kinetic assay, we used confocal microscopy to measure the MDC labeling of cyclopalladated 7a-treated yeast cells for 24 h (Fig. 10). MDC fluorescence was statistically significantly higher in yeast cells incubated with cyclopalladated 7a (Fig. 10A and B) than in controls. Together, the LTR and MDC kinetic assay results corroborated TEM images and reinforced the idea that cyclopalladated 7a induces an autophagy-like mechanism in *P. brasiliensis*.

DISCUSSION

In the present work, we showed that cyclopalladated 7a induces *Paracoccidioides* yeast cell death by at least two distinct mechanisms of action, specifically, apoptosis- and autophagy-like processes. *in vivo*, it was effective in the treatment of chronic murine PCM at low doses.

In tumor cells, cyclopalladated 7a dissipates the mitochondrial membrane potential by interacting with protein thiol groups and induces the translocation of Bax, a proapoptotic member of the Bcl-2 protein family, from the cytosol to mitochondria. In addition, cyclopalladated 7a induces an increase in the cytosolic calcium concentration and significant decreases in the ATP levels, activation of effector caspases, chromatin condensation, and DNA degradation, which are all characteristic of apoptotic intrinsic pathway activation (13). Mitochondrion-dependent apoptotic cell death was also induced by cyclopalladated 7a in leukemia cells (14), in which mitochondrial release of cytochrome *c*, caspase activation, nuclear condensation, and DNA degradation were observed. In *T. cruzi*, cyclopalladated 7a caused mitochondrial disruption (15). The participation of mitochondrial damage-initiating events that trigger apoptosis is well characterized in the literature (26).

In *P. brasiliensis* yeast cells, cyclopalladated 7a evoked mitochondrial swelling, chromatin condensation, cell membrane disruption, and accumulation of abnormal membrane structures inside vacuoles, besides chromatin condensation, an increase in superoxide anion production, an increase in metacaspase activity, and DNA degradation; all of these features corroborate the involvement of an apoptosis-like mechanism. On the other hand, cadaverin staining of autophagic acidic vacuoles suggested the involvement of an autophagy-like process related to cyclopalladated 7a. It is not the first time that both apoptosis and autophagy have been induced by the same compound. The simultaneous induction of these processes has been reported, e.g., for a curcumin analog against hepatocellular carcinoma cells (27) and by convallatoxin, an angiogenesis inhibitor (28).

This is the first time programmed cell death has been shown to occur in *Paracoccidioides*; however, it has already been described

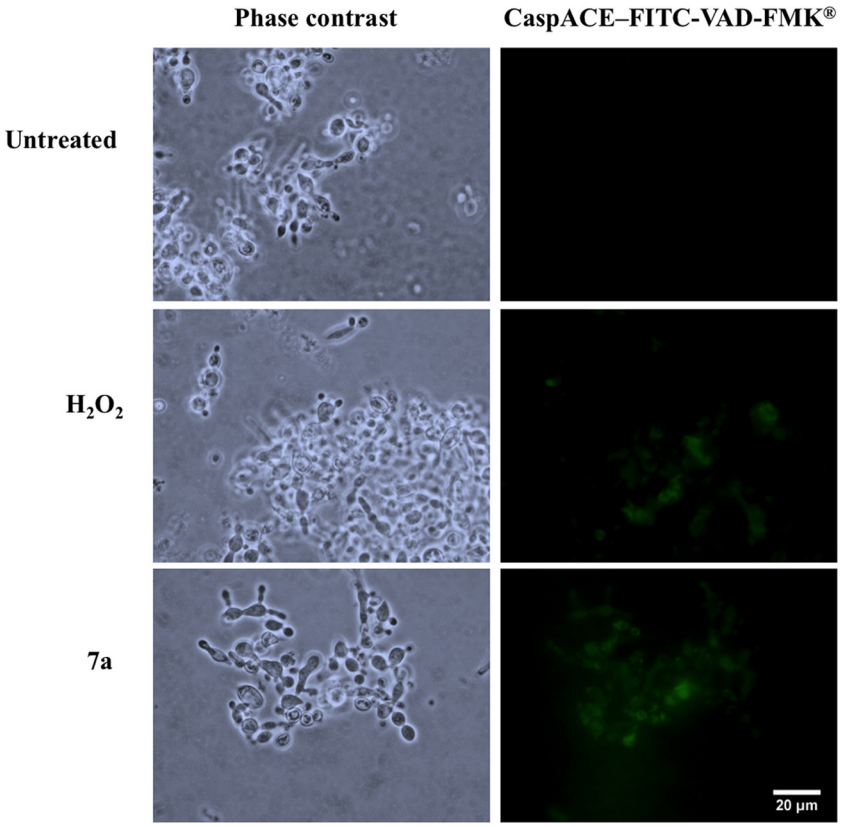

FIG 8 Cyclopalladated 7a induces metacaspase activity in *P. brasiliensis*. Pb18 yeast cells were treated with cyclopalladated 7a or H_2O_2 (positive control) or left untreated for 18 h and then stained with CaspACE–FITC-VAD-FMK. Metacaspase activity was analyzed by fluorescence microscopy. Phase-contrast images are also shown.

in other unicellular organisms, including yeast cells and bacteria (29, 30). An apoptosis-like phenotype characterized by DNA condensation and fragmentation, generation of reactive oxygen species, and phosphatidyl serine exposure was observed in *Saccharomyces cerevisiae* (31, 32), *Schizosaccharomyces pombe* (33–35), and *C. albicans* (36–38). Caspase-independent (39) and caspase-dependent intrinsic apoptosis (40) can occur in *S. cerevisiae*. Orthologs of the mammalian caspases, metacaspase Yca1p/Mca1p in *S. cerevisiae* (41) and CaMca1p in *C. albicans* (42), have been described. In *Paracoccidioides*, we found a metacaspase ortholog in each of the three genomes available: PABG_07743 in Pb3, PADG_08236 in Pb18, and PAAG_07849 in Pb01.

Autophagic cell death has not been described in *P. brasiliensis* and has rarely been reported in other fungal systems. In *S. cerevisiae*, loss of autophagy ATG genes enhanced viability (43, 44). In the present work, we observed massive cytoplasmic vacuolization in cyclopalladated 7a-treated *P. brasiliensis* that is characteristic of autophagy (45).

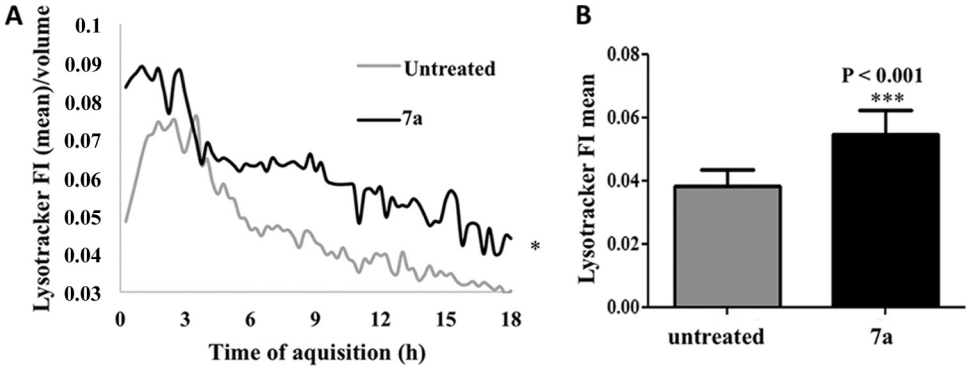

FIG 9 Cyclopalladated 7a induces vacuole acidification in *P. brasiliensis*. A LysoTracker kinetic assay was performed with live Pb18 yeast cells stained with calcofluor white and LTR DND-99 incubated with cyclopalladated 7a. (A) Relative fluorescence intensity (FI) of the LysoTracker probe contained within each calcofluor-derived isosurface normalized per unit of isosurface volume during the acquisition time. (B) Mean relative fluorescence intensity of the LysoTracker probe in cyclopalladated 7a-treated yeast cells.

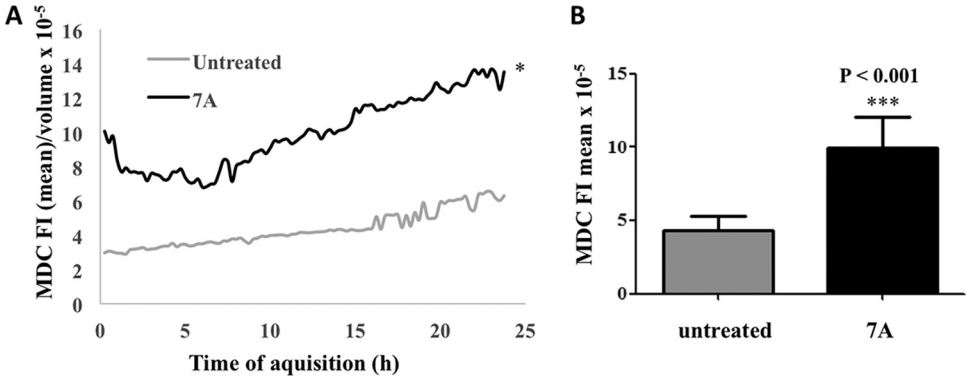

FIG 10 Cyclopalladated 7a induces an increase in autophagic vacuoles in *P. brasiliensis*. MDC kinetic assays were performed with live *P. brasiliensis* yeast cells stained with CellTracker Red CMTPx dye and MDC incubated with or without cyclopalladated 7a. (A) Relative fluorescence intensity (FI) of the MDC probe contained within each CellTracker Red CMTPx dye-derived isosurface normalized per unit of isosurface volume during the acquisition time. (B) Mean relative fluorescence intensity of the MDC probe in cyclopalladated 7a-treated yeast cells. Untreated cells were probed for comparison.

Although there are some therapeutic options available for PCM treatment, which include sulfone derivatives, amphotericin B, azoles, and terbinafine, the optimal treatment for patients with severe and disseminated forms of the disease is amphotericin B, despite its known toxic adverse effects, mainly nephrotoxicity (1). During usually long antifungal therapies, tissue damage, fibrosis, and impairment of organ functions are intensified (46), with high rates of noncompliance, relapses, and sequelae. Although alternative therapeutic approaches have been described, such as DNA vaccine (47) and nanostructured drug formulations (48), there is still a need for new drugs that are able to decrease the treatment time, toxic side effects, and sequelae.

We show here that cyclopalladated 7a is effective against *P. brasiliensis* isolates *in vitro* and *in vivo* at low concentrations, with low toxicity, and that it is able not only to decrease the *P. brasiliensis* fungal burden in the lungs of treated mice but also to diminish the lung tissue damage caused by the immune response to fungal proliferation. Therefore, cyclopalladated 7a is a promising drug to be studied further in human PCM and other mycoses, considering that it also reduced *in vitro* CFU counts of *C. albicans* and *C. neoformans* yeast cells.

ACKNOWLEDGMENTS

We thank Rita Sinigaglia Coimbra and Renato Arruda Mortara for TEM and confocal images, respectively.

We thank the Brazilian agencies FAPESP, CAPES, and CNPq for financial support.

REFERENCES

1. **Bocca AL, Amaral AC, Teixeira MM, Sato PK, Shikanai-Yasuda MA, Soares Felipe MS.** 2013. Paracoccidioidomycosis: eco-epidemiology, taxonomy and clinical and therapeutic issues. Future Microbiol **8:**1177–1191. http://dx.doi.org/10.2217/fmb.13.68.
2. **Fortes MR, Miot HA, Kurokawa CS, Marques ME, Marques SA.** 2011. Immunology of paracoccidioidomycosis. An Bras Dermatol **86:**516–524. http://dx.doi.org/10.1590/S0365-05962011000300014.
3. **Cavalcante Rde S, Sylvestre TF, Levorato AD, de Carvalho LR, Mendes RP.** 2014. Comparison between itraconazole and cotrimoxazole in the treatment of paracoccidiodomycosis. PLoS Negl Trop Dis **8:**e2793. http://dx.doi.org/10.1371/journal.pntd.0002793.
4. **Borges SR, Silva GM, Chambela Mda C, Oliveira Rde V, Costa RL, Wanke B, Valle AC.** 2014. Itraconazole vs. trimethoprim-sulfamethoxazole: a comparative cohort study of 200 patients with paracoccidioidomycosis. Med Mycol **52:**303–310. http://dx.doi.org/10.1093/mmy/myt012.
5. **Marques SA.** 2013. Paracoccidioidomycosis: epidemiological, clinical, diagnostic and treatment up-dating. An Bras Dermatol **88:**700–711. http://dx.doi.org/10.1590/abd1806-4841.20132463.
6. **Chellat F, Merhi Y, Moreau A, Yahia L.** 2005. Therapeutic potential of nanoparticulate systems for macrophage targeting. Biomaterials **26:**7260–7275. http://dx.doi.org/10.1016/j.biomaterials.2005.05.044.
7. **Sylvestre TF, Franciscone Silva LR, Cavalcante Rde S, Moris DV, Venturini J, Vicentini AP, de Carvalho LR, Mendes RP.** 2014. Prevalence and serological diagnosis of relapse in paracoccidioidomycosis patients. PLoS Negl Trop Dis **8:**e2834. http://dx.doi.org/10.1371/journal.pntd.0002834.
8. **Travassos LR, Taborda CP.** 2012. Paracoccidioidomycosis vaccine. Hum Vaccin Immunother **8:**1450–1453. http://dx.doi.org/10.4161/hv.21283.
9. **Ribeiro AM, Bocca AL, Amaral AC, Faccioli LH, Galetti FC, Zarate-Blades CR, Figueiredo F, Silva CL, Felipe MS.** 2009. DNAhsp65 vaccination induces protection in mice against *Paracoccidioides brasiliensis* infection. Vaccine **27:**606–613. http://dx.doi.org/10.1016/j.vaccine.2008.10.022.
10. **Muñoz JE, Luft VD, Amorim J, Magalhaes A, Thomaz L, Nosanchuk JD, Travassos LR, Taborda CP.** 2014. Immunization with P10 peptide increases specific immunity and protects immunosuppressed BALB/c mice infected with virulent yeasts of *Paracoccidioides brasiliensis*. Mycopathologia **178:**177–188. http://dx.doi.org/10.1007/s11046-014-9801-1.
11. **Navarro-Ranninger C, Lopez-Solera I, Perez JM, Rodriguez J, Garcia-Ruano JL, Raithby PR, Masaguer JR, Alonso C.** 1993. Analysis of two cycloplatinated compounds derived from *N*-(4-methoxyphenyl)-alpha-benzoylbenzylidenamine. Comparison of the activity of these compounds with other isostructural cyclopalladated compounds. J Med Chem **36:**3795–3801.
12. **Rodrigues EG, Silva LS, Fausto DM, Hayashi MS, Dreher S, Santos EL, Pesquero JB, Travassos LR, Caires AC.** 2003. Cyclopalladated compounds as chemotherapeutic agents: antitumor activity against a murine melanoma cell line. Int J Cancer **107:**498–504. http://dx.doi.org/10.1002/ijc.11434.
13. **Serrano FA, Matsuo AL, Monteforte PT, Bechara A, Smaili SS, Santana DP, Rodrigues T, Pereira FV, Silva LS, Machado J, Jr, Santos EL, Pesquero JB, Martins RM, Travassos LR, Caires AC, Rodrigues EG.** 2011. A cyclopalladated complex interacts with mitochondrial membrane thiol-groups and induces the apoptotic intrinsic pathway in murine and cisplatin-resistant human tumor cells. BMC Cancer **11:**296. http://dx.doi.org/10.1186/1471-2407-11-296.
14. **Guimaraes-Correa AB, Crawford LB, Figueiredo CR, Gimenes KP, Pinto LA, Grassi MF, Feuer G, Travassos LR, Caires AC, Rodrigues EG, Marriott SJ.** 2011. C7a, a biphosphinic cyclopalladated compound, efficiently controls the development of a patient-derived xenograft model of adult T cell leukemia/lymphoma. Viruses **3:**1041–1058. http://dx.doi.org/10.3390/v3071041.
15. **Matsuo AL, Silva LS, Torrecilhas AC, Pascoalino BS, Ramos TC, Rodrigues EG, Schenkman S, Caires AC, Travassos LR.** 2010. *in vitro* and *in vivo* trypanocidal effects of the cyclopalladated compound 7a, a drug

candidate for treatment of Chagas' disease. Antimicrob Agents Chemother **54:**3318–3325. http://dx.doi.org/10.1128/AAC.00323-10.
16. **Vallejo MC, Matsuo AL, Ganiko L, Medeiros LC, Miranda K, Silva LS, Freymuller-Haapalainen E, Sinigaglia-Coimbra R, Almeida IC, Puccia R.** 2011. The pathogenic fungus *Paracoccidioides brasiliensis* exports extracellular vesicles containing highly immunogenic α-galactosyl epitopes. Eukaryot Cell **10:**343–351. http://dx.doi.org/10.1128/EC.00227-10.
17. **Carvalho KC, Ganiko L, Batista WL, Morais FV, Marques ER, Goldman GH, Franco MF, Puccia R.** 2005. Virulence of *Paracoccidioides brasiliensis* and gp43 expression in isolates bearing known PbGP43 genotype. Microbes Infect **7:**55–65. http://dx.doi.org/10.1016/j.micinf.2004.09.008.
18. **Taborda CP, Nakaie CR, Cilli EM, Rodrigues EG, Silva LS, Franco MF, Travassos LR.** 2004. Synthesis and immunological activity of a branched peptide carrying the T-cell epitope of gp43, the major exocellular antigen of *Paracoccidioides brasiliensis*. Scand J Immunol **59:**58–65. http://dx.doi.org/10.1111/j.0300-9475.2004.01359.x.
19. **Real F, Mortara RA.** 2012. The diverse and dynamic nature of *Leishmania parasitophorous* vacuoles studied by multidimensional imaging. PLoS Negl Trop Dis **6:**e1518. http://dx.doi.org/10.1371/journal.pntd.0001518.
20. **Matute DR, McEwen JG, Puccia R, Montes BA, San-Blas G, Bagagli E, Rauscher JT, Restrepo A, Morais F, Nino-Vega G, Taylor JW.** 2006. Cryptic speciation and recombination in the fungus *Paracoccidioides brasiliensis* as revealed by gene genealogies. Mol Biol Evol **23:**65–73.
21. **Marques AF, da Silva MB, Juliano MA, Travassos LR, Taborda CP.** 2006. Peptide immunization as an adjuvant to chemotherapy in mice challenged intratracheally with virulent yeast cells of *Paracoccidioides brasiliensis*. Antimicrob Agents Chemother **50:**2814–2819. http://dx.doi.org/10.1128/AAC.00220-06.
22. **Arruda DC, Santos LC, Melo FM, Pereira FV, Figueiredo CR, Matsuo AL, Mortara RA, Juliano MA, Rodrigues EG, Dobroff AS, Polonelli L, Travassos LR.** 2012. β-Actin-binding complementarity-determining region 2 of variable heavy chain from monoclonal antibody C7 induces apoptosis in several human tumor cells and is protective against metastatic melanoma. J Biol Chem **287:**14912–14922. http://dx.doi.org/10.1074/jbc.M111.322362.
23. **Kajiwara K, Muneoka T, Watanabe Y, Karashima T, Kitagaki H, Funato K.** 2012. Perturbation of sphingolipid metabolism induces endoplasmic reticulum stress-mediated mitochondrial apoptosis in budding yeast. Mol Microbiol **86:**1246–1261. http://dx.doi.org/10.1111/mmi.12056.
24. **Bampton ET, Goemans CG, Niranjan D, Mizushima N, Tolkovsky AM.** 2005. The dynamics of autophagy visualized in live cells: from autophagosome formation to fusion with endo/lysosomes. Autophagy **1:**23–36. http://dx.doi.org/10.4161/auto.1.1.1495.
25. **Biederbick A, Kern HF, Elsasser HP.** 1995. Monodansylcadaverine (MDC) is a specific in vivo marker for autophagic vacuoles. Eur J Cell Biol **66:**3–14.
26. **Vaux DL, Strasser A.** 1996. The molecular biology of apoptosis. Proc Natl Acad Sci U S A **93:**2239–2244. http://dx.doi.org/10.1073/pnas.93.6.2239.
27. **Zhou T, Ye L, Bai Y, Sun A, Cox B, Liu D, Li Y, Liotta D, Snyder JP, Fu H, Huang B.** 2014. Autophagy and apoptosis in hepatocellular carcinoma induced by EF25-(GSH)2: a novel curcumin analog. PLoS One **9:**e107876. http://dx.doi.org/10.1371/journal.pone.0107876.
28. **Yang SY, Kim NH, Cho YS, Lee H, Kwon HJ.** 2014. Convallatoxin, a dual inducer of autophagy and apoptosis, inhibits angiogenesis in vitro and in vivo. PLoS One **9:**e91094. http://dx.doi.org/10.1371/journal.pone.0091094.
29. **Engelberg-Kulka H, Amitai S, Kolodkin-Gal I, Hazan R.** 2006. Bacterial programmed cell death and multicellular behavior in bacteria. PLoS Genet **2:**e135. http://dx.doi.org/10.1371/journal.pgen.0020135.
30. **Bayles KW.** 2007. The biological role of death and lysis in biofilm development. Nat Rev Microbiol **5:**721–726. http://dx.doi.org/10.1038/nrmicro1743.
31. **Madeo F, Frohlich E, Frohlich KU.** 1997. A yeast mutant showing diagnostic markers of early and late apoptosis. J Cell Biol **139:**729–734. http://dx.doi.org/10.1083/jcb.139.3.729.
32. **Madeo F, Frohlich E, Ligr M, Grey M, Sigrist SJ, Wolf DH, Frohlich KU.** 1999. Oxygen stress: a regulator of apoptosis in yeast. J Cell Biol **145:**757–767. http://dx.doi.org/10.1083/jcb.145.4.757.
33. **Ink B, Zornig M, Baum B, Hajibagheri N, James C, Chittenden T, Evan G.** 1997. Human Bak induces cell death in *Schizosaccharomyces pombe* with morphological changes similar to those with apoptosis in mammalian cells. Mol Cell Biol **17:**2468–2474.
34. **Jürgensmeier JM, Krajewski S, Armstrong RC, Wilson GM, Oltersdorf T, Fritz LC, Reed JC, Ottilie S.** 1997. Bax- and Bak-induced cell death in the fission yeast *Schizosaccharomyces pombe*. Mol Biol Cell **8:**325–339. http://dx.doi.org/10.1091/mbc.8.2.325.
35. **Torgler CN, de Tiani M, Raven T, Aubry JP, Brown R, Meldrum E.** 1997. Expression of bak in *S. pombe* results in a lethality mediated through interaction with the calnexin homologue Cnx1. Cell Death Differ **4:**263–271. http://dx.doi.org/10.1038/sj.cdd.4400239.
36. **Phillips AJ, Sudbery I, Ramsdale M.** 2003. Apoptosis induced by environmental stresses and amphotericin B in *Candida albicans*. Proc Natl Acad Sci U S A **100:**14327–14332. http://dx.doi.org/10.1073/pnas.2332326100.
37. **Ramsdale M.** 2008. Programmed cell death in pathogenic fungi. Biochim Biophys Acta **1783:**1369–1380. http://dx.doi.org/10.1016/j.bbamcr.2008.01.021.
38. **Hao B, Cheng S, Clancy CJ, Nguyen MH.** 2013. Caspofungin kills *Candida albicans* by causing both cellular apoptosis and necrosis. Antimicrob Agents Chemother **57:**326–332. http://dx.doi.org/10.1128/AAC.01366-12.
39. **Liang Q, Li W, Zhou B.** 2008. Caspase-independent apoptosis in yeast. Biochim Biophys Acta **1783:**1311–1319. http://dx.doi.org/10.1016/j.bbamcr.2008.02.018.
40. **Mazzoni C, Falcone C.** 2008. Caspase-dependent apoptosis in yeast. Biochim Biophys Acta **1783:**1320–1327. http://dx.doi.org/10.1016/j.bbamcr.2008.02.015.
41. **Uren AG, O'Rourke K, Aravind LA, Pisabarro MT, Seshagiri S, Koonin EV, Dixit VM.** 2000. Identification of paracaspases and metacaspases: two ancient families of caspase-like proteins, one of which plays a key role in MALT lymphoma. Mol Cell **6:**961–967. http://dx.doi.org/10.1016/S1097-2765(05)00086-9.
42. **Cao Y, Huang S, Dai B, Zhu Z, Lu H, Dong L, Wang Y, Gao P, Chai Y, Jiang Y.** 2009. *Candida albicans* cells lacking CaMCA1-encoded metacaspase show resistance to oxidative stress-induced death and change in energy metabolism. Fungal Genet Biol **46:**183–189. http://dx.doi.org/10.1016/j.fgb.2008.11.001.
43. **Dziedzic SA, Caplan AB.** 2011. Identification of autophagy genes participating in zinc-induced necrotic cell death in *Saccharomyces cerevisiae*. Autophagy **7:**490–500. http://dx.doi.org/10.4161/auto.7.5.14872.
44. **Dziedzic SA, Caplan AB.** 2012. Autophagy proteins play cytoprotective and cytocidal roles in leucine starvation-induced cell death in *Saccharomyces cerevisiae*. Autophagy **8:**731–738. http://dx.doi.org/10.4161/auto.19314.
45. **Galluzzi L, Vitale I, Abrams JM, Alnemri ES, Baehrecke EH, Blagosklonny MV, Dawson TM, Dawson VL, El-Deiry WS, Fulda S, Gottlieb E, Green DR, Hengartner MO, Kepp O, Knight RA, Kumar S, Lipton SA, Lu X, Madeo F, Malorni W, Mehlen P, Nunez G, Peter ME, Piacentini M, Rubinsztein DC, Shi Y, Simon HU, Vandenabeele P, White E, Yuan J, Zhivotovsky B, Melino G, Kroemer G.** 2012. Molecular definitions of cell death subroutines: recommendations of the Nomenclature Committee on Cell Death 2012. Cell Death Differ **19:**107–120. http://dx.doi.org/10.1038/cdd.2011.96.
46. **Benard G, Campos AF, Netto LC, Goncalves LG, Machado LR, Mimicos EV, Franca FO, Gryschek RC.** 2012. Treatment of severe forms of paracoccidioidomycosis: is there a role for corticosteroids? Med Mycol **50:**641–648. http://dx.doi.org/10.3109/13693786.2011.654135.
47. **Pinto AR, Puccia R, Diniz SN, Franco MF, Travassos LR.** 2000. DNA-based vaccination against murine paracoccidioidomycosis using the gp43 gene from *Paracoccidioides brasiliensis*. Vaccine **18:**3050–3058. http://dx.doi.org/10.1016/S0264-410X(00)00074-8.
48. **Kleinberg M.** 2006. What is the current and future status of conventional amphotericin B? Int J Antimicrob Agents **27**(Suppl 1)**:**12–16. http://dx.doi.org/10.1016/j.ijantimicag.2006.03.013.